Review

Allosteric kinase inhibitors: a new paradigm for effective and selective modulation of kinase activities

Hongliang Yang, Ting Chen, Xu Bai, Yazhong Pei*

The Center for Combinatorial Chemistry and Drug Discovery, School of Pharmaceutical Sciences, Jilin University, Changchun 130021, China

Abstract: Dysregulation of kinases has been proven to be one of the main causes of abnormal growth and survival of cancer cells. Selective modulations of kinase activities have become the focus of many research programs for the development of safe and effective chemotherapy for cancers. So far, fifteen kinase inhibitors have received FDA approval for the treatment of various forms of cancers. Among them, the allosteric kinase inhibitors have been shown to have superior clinical profile in terms of safety and efficacy. In this review, we summarize the allosteric conformations of kinases, their corresponding inhibitors and the modes of their interactions.

Keywords: Protein kinase; Allosteric conformation; DFG-out; ATP non-competitive; Kinase inhibitor

CLC number: R962.1 **Document code:** A **Article ID:** 1003−1057(2012)6−531−13

Contents

1. Introduction

Protein kinases catalyze the transfer of the terminal phosphoryl group of ATP to specific hydroxyl groups of serine, threonine or tyrosine residues of their protein substrates. This phosphorylation turns on (in most cases) or off the substrate proteins' catalytic activity, thus, play pivotal roles in regulating almost all aspects of cellular functions[1]. The dysregulations of kinases have been implicated in a number of disease areas ranging from neuronal disorders to oncology. For these reasons, protein kinases have become one of the most comprehensive classes of therapeutic targets, which amounted to about a quarter of global pharmaceutical research efforts. Most successes have been achieved in the field of cancer research. In recent years, several small molecule kinase inhibitors have been marketed as anti-cancer agents, including BCR/ABL inhibitors imatinib, nilotinib and desatinib; EGFR inhibitors gefitinib, erlotinib and lapatinib; VEGFR inhibitors sorafenib, sunitinib, pegaptanib, pazopanib, vandetanib and axitinib; B-Raf inhibitor vemurafanib; Jak inhibitor ruxolitinib and ALK/cMet inhibitor critozinib. Currently, numerous small molecules targeting kinases are in various development stages, and being continuously advanced into the clinics[2].

Small molecules can affect the activities of kinases by various ways, and the mechanisms of action for some of them are not yet well understood. Most of the kinase inhibitors reported so far can be classified into two main categories based on their mode of actions: Type 1 and Type 2 kinase inhibitors[3]. Type 1 inhibitors bind to the ATP site of the kinase's active conformation by forming 1–3 H-bonds with the hinge region of the kinase, similar to the binding mode of the adenine residue of the ATP. They modulate the kinase activity by directly competing with ATP for the same binding site. They tend to exhibit much higher potency in biochemical assays (low ATP concentration) than in

Received date: 2012-06-27.
*Corresponding author. Tel.: 86-431-85619260;
E-mail: peiyz@jlu.edu.cn

doi:10.5246/jcps.2012.06.068

cellular assays (high ATP concentration). Characteristically, their measured IC_{50} values in biochemical assays will increase with the escalation of the ATP concentration in the testing media. For this reason, they are also termed as "ATP-competitive inhibitors". The amino acid sequences in the ATP binding sites are highly conserved among kinases and other ATP binding proteins. As a result, in general, Type 1 inhibitors exhibit poor selectivity profile, unless they can present diverse functionalities to the regions adjacent to the ATP site to achieve target specific interactions. In contrast, Type 2 inhibitors bind to the kinases in locations that are away from the ATP and the substrate sites (allosteric sites); they induce a conformational change of the kinase to render it inactive. One common allosteric site is created by the kinase activation loops assuming a different conformation, in which the highly conserved DFG motif rotated out and placed the phenylalanine residue about 10 Å away from its position required for phosphate transfer from the ATP to the substrates[4]. This inactive conformation was also termed as the DFG-out conformation, which exposed an additional hydrophobic pocket adjacent to the ATP pocket that is frequently referred to as the "allosteric site". This has been shown to be the common binding mode of several recently reported inhibitors targeting various kinases. Compounds that bind to the allosteric site and render the target kinase inactive are classified as Type 2 inhibitors[1]. So far, all the X-ray data show only kinases with non-phosphorylated activation-loop co-crystallized with Type 2 inhibitors. The interaction between Type 2 inhibitor and phosphorylated kinase (activated form) remains unclear. Most likely, Type 2 inhibitors shift the equilibrium between active and the DFG-out conformations by inducing and stabilizing the relatively high energetic DFG-out form. This can either prevent the phosphorylation of the activation-loop by upstream kinases or facilitate the dephosphorylation by phosphatases. The former seems to be a more likely scenario since Type 2 inhibitors, in general, show weak or no activity against phosphorylated kinases in biochemical assays in which phosphatases are absent. Because the amino acid residues in and around this DFG-out allosteric site are less conserved than the ATP site, it has been proposed that high kinase selectivity may be easier to achieve for Type 2 inhibitors. Because the DFG-out conformation has much lower affinity for ATP, Type 2 inhibitors typically cannot be displaced by ATP. Therefore, their potencies in biochemical assays are not affected by the ATP concentrations in the testing media. This method has been routinely used to distinguish Type 1 and Type 2 inhibitors, in addition to X-ray co-crystallography techniques. This non-ATP competitive nature of Type 2 inhibitors make them more efficacious in cell based and in vivo assays, since they do not need to compete with the high concentration of the ATP under these conditions. This may also translate to the better efficacy observed in the clinics with marketed Type 2 inhibitors such as imatinib and others.

In this review, we summarize the Type 2 inhibitors whose modes of action have been confirmed using X-ray co-crystallography or shown to modulate kinase activities in a non-ATP competitive fashion. Some kinase inhibitors bind to their targets at an allosteric site which is different from the DFG-out conformations and render the kinases inactive are also included. This review will focus on the key interactions between the allosteric conformations of kinases and their small molecule ligands, and the common features of the inhibitor-kinase complex within each kinase family. A systematic analysis of this type of information is a worthwhile exercise for the design of next generation Type 2 kinase inhibitors with improved efficacy and safety profiles.

2. Allosteric kinase inhibitors

2.1. Bcr-Abl kinase inhibitors

The ubiquitous non-receptor tyrosine kinase, c-Abl was one of the first kinases as drug development target in oncology. It has been shown to play an essential role in cell signal transduction, balancing events leading to apoptosis or to increased cell proliferation. The critical role of c-Abl kinase in cell proliferation is illustrated by the dramatic manifestation of chronic myelogenous leukemia (CML) due to over expression of Bcr-Abl, a kinase-activated mutant form of c-Abl tyrosine kinase.

Imatinib (Table 1) is a potent inhibitor of Bcr-Abl with a reported IC_{50} of 10.8 nM in an enzymatic assay[4]. It was the first successfully marketed kinase inhibitor for the treatment of CML by Novartis in 2001. X-ray co-crystallography study revealed that in the complex of c-Abl and imatinib, the kinase has adopted a confirmation that is different from its active form. In this new conformation, the activation loop of the kinase rotated about 180 degrees and the highly conserved DFG motif in the activation loop is 10 Å away from its normal location[5]. As shown in Figure 1, imatinib is sandwiched between the *N*- and *C*-lobes of the kinase domain and penetrates through the central region of the kinase. Its piperazinylphenyl fragment occupies the newly created allosteric site. Its amide linker forms two key H-bonds with the Glu286 and the DFG-motif. The amino-pyrimidinylpyridine extends into the site where the adenine ring of the ATP normally binds and forms two additional H-bonds with the hinge. In total, the compound makes six hydrogen bonds with the protein, and the majority of contacts are mediated by hydrophobic van der Waals interactions. It was later found that several other kinases can also assume similar inactive "DFG-out" conformations due to the rotation of their activation loop. The success of imatinib indicates this type of allosteric sites can be exploited for the development of potent and selective kinase inhibitors.

Since the launch of imatinib, many drug resistant Bcr-Abl mutants have been identified in the clinics, and the search for more efficacious Bcr-Abl inhibitors with wider application for the treatment of CML continued. Nilotinib (also been called AMN107, Table 1) is a second generation Bcr-Abl kinase inhibitor structurally similar to imatinib. Its left portion (pyridinyl-pyrimidinylamino-tolyl) is identical to that of imatinib while the orientation of the amide linker is reversed and the substitutions of the phenyl ring on the right side are modified. These modifications allowed

Table 1. Allosteric inhibitors of Bcr-Abl kinase

Comp.	Anonym	Structure	Target IC_{50} (nM)[a]	Status	Institute
1	Imatinib	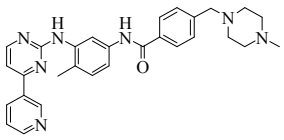	10.8	Marketed	Novartis
2	Nilotinib	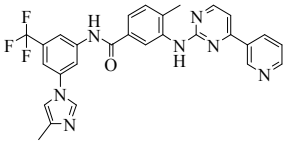	20–60	Marketed	Novartis
3	GNF-6	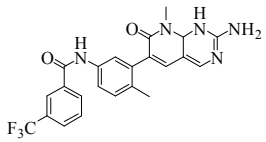	243	Preclinical	Novartis
4	GNF-7	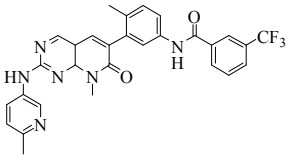	297	Preclinical	Novartis
5	GNF-2	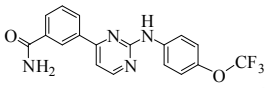	267	Preclinical	Novartis
6	GNF-5	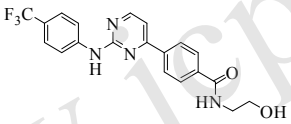	NA[b]	Preclinical	Novartis

[a] Enzymatic activity assay; [b] Not available.

nilotinib to bind to the inactive DFG-out conformation of Bcr-Abl in a similar fashion as imatinib, also afforded nilotinib with higher affinity towards Bcr-Abl and wider clinical applicability[6]. Nilotinib is 10 to 50 fold more potent than imatinib against Bcr-Abl and also shows efficacy against many imatinib-resistant mutants. Nilotinib was approved by the FDA in 2007 for the treatment of CML with patients who become resistant to imatinib or in an advanced stage of the disease.

Although nilotinib and ATP-competitive inhibitor dasatinib have shown improved efficacy against many of the Bcr-Abl mutants, one mutant, the so-called "Gatekeeper" T315I, remained to be a challenge. New generation Type 2 Bcr-Abl inhibitor GNF-7 was a hybrid of Type 1 and Type 2 inhibitor. It utilizes more ATP-binding site to pick up more H-bond interactions to achieve higher affinity, but still induce the DFG-out conformation around the active site. GNF-7 has been shown to be able to inhibit both the wild-type and T315I mutant Bcr-Abl activity in biochemical and cellular assays[7]. GNF-7 exhibits potent inhibitory activity against other clinically relevant Bcr-Abl mutants including G250E, Q252H, Y253H, E255K, E255V, F317L and M351T. GNF-7 has also been shown to be efficacious against T315I-Bcr-Abl dependent tumor growth in a murine model of CML[7]. GNF-6, a close analogue of GNF-7, has been co-crystallized with Abl kinase (Fig. 2) and is shown to bind to the kinase in a similar mode as that of imatinib and nilotinib but extend more into the ATP site for additional H-bonding with the hinge and avoids the H-bond interaction with gatekeeper moieties[8].

Recently, GNF-2 has been confirmed, by both NMR and X-ray co-crystal data, to bind to the myristate site of c-Abl that is 30 Å away from the active site and induces a conformational change in helix α I that stabilizes the auto-inhibited form of Bcr-Abl (Fig. 3). GNF-2 exhibits similar potency against Bcr-Abl transformed cells when compared with imatinib. GNF-5 is a close derivative of GNF-2 where the benzamide is *N*-substituted with hydroxyethyl to improve its pharmacokinetic properties. GNF-5, when used in combination with imatinib or nilotinib, was able to suppress the emergence of resistance mutations in vitro and showed additive inhibitory activity in biochemical and cellular assays against T315I mutant human Bcr-Abl. In a murine bone-marrow transplantation model, the combination of GNF-5 and imatinib or nilotinib showed good efficacy against this recalcitrant mutant. These results indicate that allosteric binding to the myristate site can produce therapeutically relevant inhibition of Bcr-Abl activity, and combination therapies with other inhibitors can overcome resistance to either agent alone[6].

Figure 1. X-ray co-crystal structure of imatinib bind to Bcr-Abl kinase (PDB ID 2HYY)[5]. The activation loops and the van der Waals surfaces corresponding to the inhibitors are colored blue for imatinib. The DFG motif situated at the NH_2 terminus of the activation loop is colored gold. Helix αC and the interlobe connector are colored dark green.

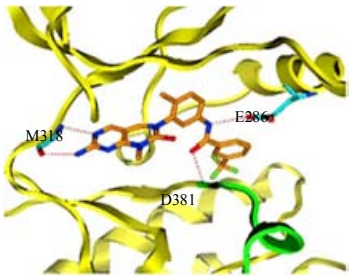

Figure 2. X-ray co-crystal structure of GNF-6 (gold) binds to Bcr-Abl kinase (yellow ribbon)[8].

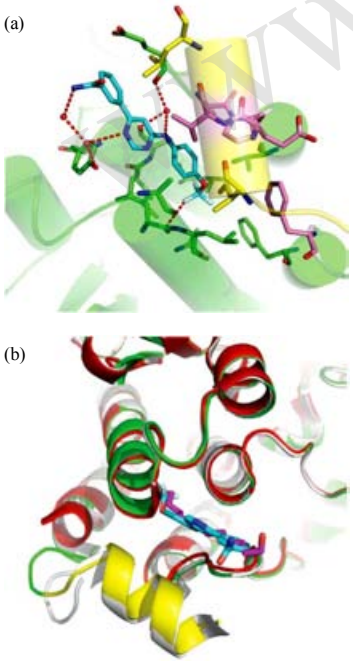

Figure 3. X-ray co-crystal structure of GNF-2 binds to Bcr-Abl (PDB accession 1OPK)[9]. (a) Abl kinase is indicated in green (helices are indicated by transparent cylinders), with the bent part of the I-helix in yellow, GNF-2 resistance mutations in pink, and GNF-2 carbons in cyan. Hydrogen bonding and other polar interactions are indicated by dotted red lines; (b) Superposition of the Abl/imatinib/myristate (white), Abl/imatinib/GNF-2 (green and yellow) and Abl-imatinib (red) structures. GNF-2 is coloured in cyan, and myristic acid in magenta.

2.2. Mitogen-activated protein kinases (MAPKs) inhibitors

MAPKs play important roles in the transduction of extracellular stimuli to the nucleus triggering cellular events in response to changes in the surrounding environment. The dysregulation of MAPK pathway has been implicated in many disease conditions, especially in inflammation and cancer. Among the MAPK signaling cascades, three classes of kinases, including p38 kinases, c-Jun *N*-terminal kinase (JNK) and the extracellular signal-regulated kinase (ERK), have been shown to be the pivotal parts of the MAPK network and are the therapeutic targets for numerous drug development efforts.

2.2.1. P38 kinase inhibitors

P38 are intracellular serine/threonine (Ser/Thr) kinases that exist in four isoforms p38α, p38β, SAPK3/p38γ and SAPK4/p38δ. Data show p38 isoforms have different distribution patterns within the body and may have different biological functions and physiological substrates. But all of them phosphorylate substrates containing the minimal consensus sequence Ser-Pro or Thr-Pro. Among them, p38α, which is activated by a range of environmental stimuli such as TNF-α, IL-1β and stress, has attracted the most attention for drug development. Its over-expression and/or hyperactivity have been implicated in inflammation, pain, cancer and various autoimmune disorders. Allosteric inhibitors of p38 kinase are listed in Table 2.

BIRB796 is a potent p38α inhibitor developed from a series of diarylureas which was initially identified through high-throughput screening. The X-ray crystallography (Fig. 4) showed BIRB796 binds to an inactive DFG-out conformation of p38 with the phenylalanine residue shifting 10 Å away from the hydrophobic-binding pocket, which created a new hydrophobic-binding pocket adjacent to the ATP-binding site for the insertion of the *tert*-butyl substituent of BIRB796. The tolyl substituent on the pyrazole forces a conformational change in the Glu71 side chain and picks up a favorable hydrophobic interaction with lipophilic portion of the side chain. The urea moiety forms two H-bonds with the terminal carboxylates of Glu71 and Asp168. The naphthal ring occupies the kinase specificity pocket and also picks up a lipophilic interaction with Phe169 of the DFG-motif. The morpholino substituent extends into the ATP pocket and forms an H-bond with the Met109. Although BIRB796 selectively inhibits the p38α MAPK isoform, blocks TNFα release in vitro and inhibits collagen-induced arthritis in vivo, its use in phase 2 clinical trials for rheumatoid arthritis, psoriasis and Crohn's disease was compromised by its liver toxicity[10,11].

Since the publication of BIRB796 and its DFG-out binding mode to the p38α kinase, allosteric inhibition of p38 kinase activity has been the focus of many research programs. A report from AstraZeneca described 6-(methyl-anilino) quinazolines (compound **8**) as potent and selective inhibitors of the p38α MAPK kinase signaling pathway in vitro and in vivo. X-ray co-crystal structure reveals that the quinazoline N1 also forms a hydrogen bond with the backbone amide NH of Met109 and the aniline ring buried into the hydrophobic region formed by the carbon atoms of residues

including Lys53 and Thr106 (Fig. 5). The amide linker of compound **8** forms two hydrogen bonds with the carboxylate side chain of Glu71 and the backbone amide NH of Asp168. The 2-pyrrolidinylethoxy group of compound **8** points out towards the solvent and has weak electron density in the structure suggesting it has unrestricted movement[12].

Two compounds disclosed by Astex, compound **9** and compound **10**, also were able to induce the conformational change of the DFG motif in the p38 activation loop. X-ray co-crystal structures shows that the Phe169 side chain has again moved approximately 10 Å to a new DFG-out conformation, whereby the Phe169 side chain now shields access to the ATP binding site. Asp168 and Glu71 form a polar channel between the ATP binding site and this allosteric pocket, which is involved in a hydrogen bond network to both the amide and urea functionalities. This movement of the Phe169 side chain exposes a large lipophilic pocket into which the morpholine of compound **9** or the *tert*-butyl group of compound **10** may then insert (Fig. 6). The morpholine and *tert*-butyl moieties, respectively, make substantial contacts with a number of neighboring hydrophobic residues, both **9** and **10** still maintain contacts to the hinge and lipophilic specificity pockets[13].

BMS recently reported a series of pyrrolo[1,2-*f*][1,2,4] triazine derivatives as potent and selective p38α MAPK

Table 2. Allosteric inhibitors of p38 kinase

Comp.	Anonym	Structure	Target IC_{50} (nM)[a]	Status	Institute
7	BIRB796	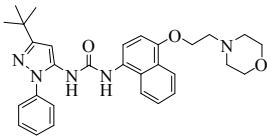	4	Phase 2	BoehringerIngelheim
8	Compound **8**	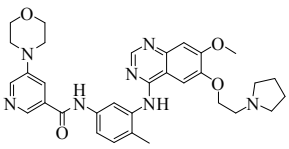	39	Preclinical	AstraZeneca
9	Compound **9**	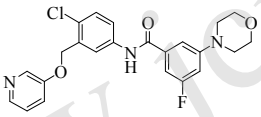	65	Preclinical	Astex
10	Compound **10**	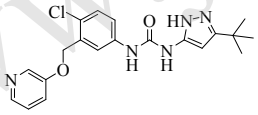	350	Preclinical	Astex
11	BMS-582949	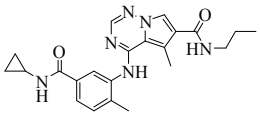	18	Phase 2	Brisyol-Myers Squibb

[a] Enzymatic activity assay.

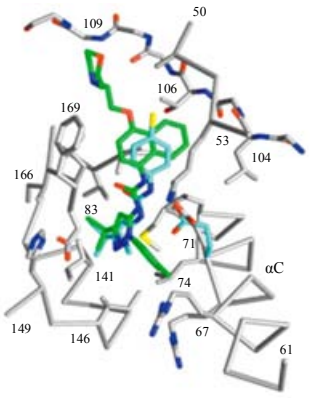

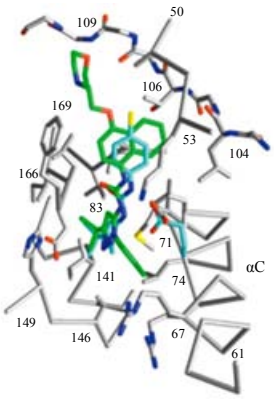

Figure 4. X-ray co-crystal structure of BIRB796 binds to p38α (PDB ID 1KV2). Stereo view showing the binding pocket (gray for carbon atoms) for BIRB796 (green)[11].

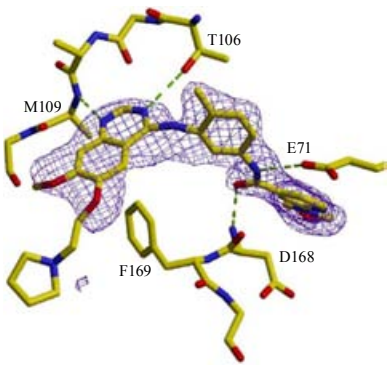

Figure 5. X-ray co-crystal structure of compound **8** binds to p38α. The electron density of compound **8** is shown in purple. Protein residues 71, 106 to 110 and 168 to 170 (the DFG motif) are shown and hydrogen bonds to compound **8** are indicated with dashed lines[12].

kinase inhibitors[14]. BMS-582949, an analogue with improved pharmaceutical properties, has been advanced into phase 2 clinical trials for the treatment of autoimmune disorders. The X-ray co-crystal data shows BMS-582949 binding to the DFG-out conformation of the p38α enzyme (Fig. 7). Its benzamide moiety forms two key hydrogen bonds with p38α: the carbonyl oxygen interaction with Asp168 and the NH interaction with Glu71. Another important hydrogen bond interaction occurs between the 6-carboxamide oxygen and the Met109 at the hinge region. Hydrophobic interactions include the angular methylaniline moiety being positioned within a hydrophobic pocket and the pendant *N*-propyl interacting with a hydrophobic site characteristically found at the outer rim of the hinge region[15].

The p38 inhibitors described above, based on different templates, all induce and bind to the DFG-out conformation of p38 in a similar fashion, utilizing the same amino acid residues for H-bonds and hydrophobic pockets for lipophilic interactions. This "induced-fit" binding mode may be associated with slow binding kinetics observed with some of those inhibitors, suggesting the structural rearrangement required for the binding event is rare. It also suggests that the DFG-out conformation is a relatively high energy state comparing to the active conformation, and is only observed when bound and stabilized with small molecule ligands.

2.2.2. Mitogen-activated proteinkinase kinase (MAPKK)

Activation of the p42/44 MAPK signaling pathway comprising mitogen-activated protein kinase/extracellular signal-regulated kinase (ERK) kinase (MEK)-ERK has been implicated in the pathogenesis and progression of various human malignant tumors[16,17]. The MEK-ERK pathway is often activated by mutation of upstream factors, BRAF or Ras, or by the signals of constitutively activated cell-surface receptors. Therefore, inhibition of the p42/44 MAPK pathway is an attractive therapeutic strategy for multiple cancers. Indeed, several small molecules that target this pathway, including MEK and Raf inhibitors, are being tested in human clinical studies[18]. Allosteric inhibitors of MAPK kinase are listed in Table 3.

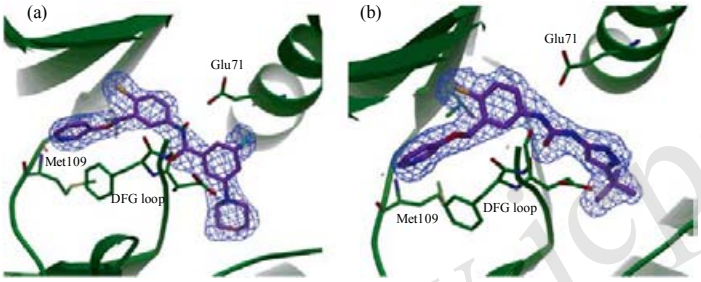

Figure 6. (a) X-ray co-crystal structure of compound **9** binds to p38α; (b) X-ray co-crystal structure of compound **10** binds to p38α[13].

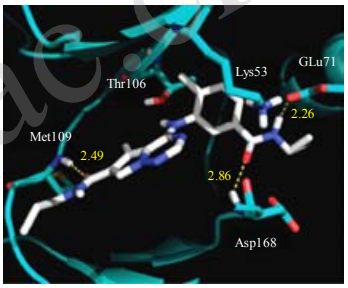

Figure 7. X-ray co-crystal structure of BMS-582949 binds to p38α[15].

Table 3. Allosteric inhibitors of MAPK kinase

Comp.	Anonym	Structure	Target IC_{50} (nM)[a]	Status	Institute
11	PD184352	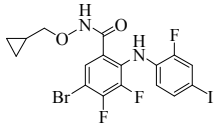	17	Phase 2	Pfizer
12	PD318088	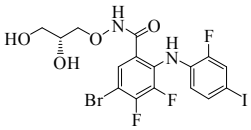	NA[b]	NA[b]	Pfizer
13	RDEA119	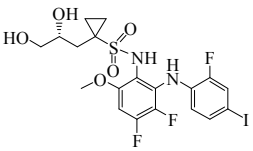	19	Phase 1	Ardea
14	TAK-733	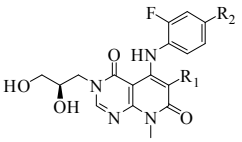	3.2	Phase 1	Takeda
15	CH4987655	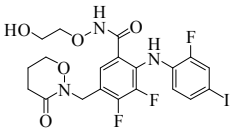	5.2	Phase 1	Kamakura

[a] Enzymatic activity assay; [b] Not available.

PD184352 was identified as a highly selective, potent inhibitor of MEK1 and MEK2 that was noncompetitive for both MgATP and MAPK. Notably, PD184352 was shown to have substantial anti-proliferative activity in vivo and was placed in clinical trials for the treatment of cancer. Its structurally closely related analogues, PD318088 and PD334581, were used in X-ray co-crystal study to determine the mechanism of their inhibitory activity against MEK1 and MEK2 kinases[19].The crystal structures of MEK1 and MEK2 were obtained as ternary complexes with MgATP and PD318088 and PD33458, respectively; and were found to be highly homologous to each other. To simplify the discussion, only the ternary complex of PD318088 with MEK1 and MgATP was discussed to illustrate the binding mode of these inhibitors. X-ray co-crystal structure shows PD318088 binds in a novel allosteric binding pocket that is adjacent to but not overlapping with the MgATP binding site (Fig. 8). The inhibitor-bound MEK enzymes are catalytically inactive for two reasons. First, the *N*-terminal region of the MEK activation loop exists in an inactive α-helical conformation that partially occludes the binding site for the ERK activation loop. Second, helix C adopts an inactive conformation wherein an important ion pair between the conserved Glu114 and the catalytic Lys97 residue in the ATP-binding site has been broken through the rotation of helix C. PD184352 and its analogues have been further evaluated in preclinical and clinical settings and have shown to be less than satisfactory in terms of safety and efficacy. The need for novel MEK inhibitors with superior efficacy and better physicochemical, metabolic and safety profiles still remains.

Recently, RDEA119 has been reported to potently inhibit MEK activity in enzyme inhibition assays in a non-ATP competitive manner (MEK1 IC_{50} = 19 nM, MEK2 IC_{50} = 47 nM) determined through incorporation of radioactive phosphate from ATP into ERK as substrate[20]. The X-ray crystal structure of RDEA119-MEK complex (Fig. 9) reveals that RDEA119 binds to an allosteric site adjacent to the Mg-ATP binding region and interacts extensively with ATP, the activation loop, and other surrounding residues through hydrogen bonding and hydrophobic interactions[20]. Notably, the sulfonamide moiety hydrogen bonds with the basic side chain of the Lys97, a conserved residue believed to be important for the catalytic activity of protein kinases. The iodine is in electrostatic interaction with backbone C=O of Val127, whereas one of the two fluorines is involved in hydrogen bonding with the -NH of Ser212. This inhibitor also forms several contacts with Asp208, Phe209, and Gly210, also known as the DFG motif that is shared across several families of protein kinases. The diol extension of RDEA119 interacts heavily with oxygen atoms of thea and phosphate groups of the ATP cofactor. RDEA119 is also engaged in hydrophobic contacts with side chains of residues Ile99, Leu115, Leu118, Phe129, Ile141, Met143, Asp190, Cys207, Asp208, Phe209, Gly210, Val211, Ser212, Leu215, and Ile216. In addition, RDEA119 has a unique cyclopropyl group that is in direct hydrophobic contacts with the side chain of Met219 in the A-loop, further stabilizing it in the closed "active" confirmation of the enzyme. Such a binding mode thus suggests a noncompetitive mechanism

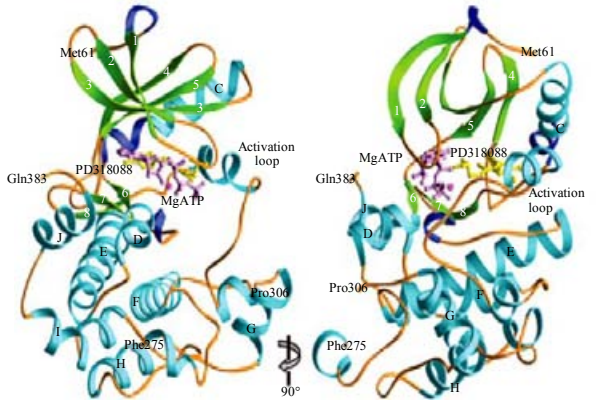

Figure 8. Detailed view of the interactions involved in orienting PD318088 and MgATP in the MEK1 structure (PDB ID 1S9). The α-helical regions of the protein are cyan, the β-sheet regions are green, the ATP cofactor is pink, the magnesium atom is magenta and PD318088 is gold[19].

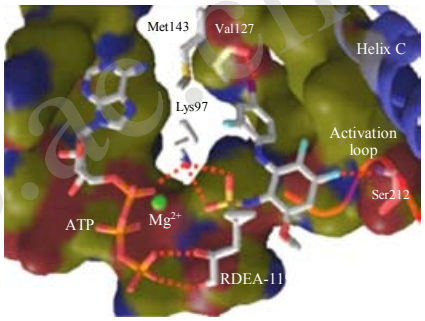

Figure 9. X-ray co-crystal structure of REDA119 binds to MEK (PDB: 3E8N).ATP, RDEA119, and representative residues of protein (i.e., Lys97, Met143, and Ser212) are represented by sticks. Atoms are colored according to type: carbon in gray, oxygen in red, nitrogen in blue, sulfur in yellow, fluorine in light blue, and iodine in purple. Red dashed lines, hydrogen bonds or electrostatic interactions[20].

of inhibition of RDEA119 against MEK1, which allows ATP binding but precludes binding to the substrate ERK, thus preventing ERK phosphorylation.

Like RDEA119, TAK-733 and CH4987655 developed by Takeda and Chugai, respectively, also structurally resemble PD318088[21,22]. As a result, they bind to and inhibit the MEK kinase in a similar fashion as that of PD318088, as shown in the X-ray co-crystal structure of their ternary complex with MEK kinase and MgATP. TAK-733 exhibited potent enzymatic and cell activity with an IC_{50} of 3.2 nM against constitutively active MEK enzyme and an EC_{50} of 1.9 nM against ERK phosphorylation in cells[21]. It was found to bind plasma protein moderately, and exhibited high permeability and high microsomal stability across species. CH4987655 is also a potent and selective MEK inhibitor, with IC_{50} of 5.2 nM in a biochemical assay, and EC_{50} in low nM range against multiple tumor cells in anti-proliferation assays[22]. It shows slow dissociation from MEK, high metabolic stability and good in vivo antitumor efficacy with clear target inhibition in tumor without distribution into the brain. CH4987655 used in combination with the PI3K/Akt/mTOR pathway inhibitor

showed enhanced in vivo efficacy, exhibiting clear tumor regression. It has been advanced into a phase 1 clinical study for the treatment of solid tumors.

2.3. Polo-like kinases inhibitor

Polo-like kinases (PLKs) regulate numerous cell cycle events including the onset of mitosis, DNA-damage checkpoint activation, regulation of the anaphase promoting complex, and centrosome duplication and maturation. Four distinct PLKs have been identified to date in mammals: PLK1, PLK2 (SNK), PLK3 (PRK and FNK), and PLK4 (FNK). The four kinases are structurally homologous with two conserved regions, an *N*-terminal catalytic kinase domain and a *C*-terminal region which is comprised of "polo boxes". Among them, PLK1 is the best characterized and is recognized to be a key component of the cell cycle control machinery with important roles in the mitotic entry, centrosome duplication, bipolar mitotic spindle formation, transition from metaphase to anaphase, cytokinesis and maintenance of genomic stability. PLK1 is overexpressed in many tumor cells, and those patients whose tumors display higher levels of PLK1 have lower survival rates than those with lower levels.

ON01910 (Fig. 10) is a small molecule non-ATP competitive inhibitor of PLK1 with an IC_{50} of 10 nM and induces mitotic arrest of tumor cells characterized by spindle abnormalities leading to their apoptosis. The compound was efficacious against tumor growth in a variety of xenograft nude mouse models, and also found to be highly effective in combination with conventional chemotherapy. The exact mode of interaction of ON01910 with PLK1 is not known. It appears to compete for the substrate binding site rather than that of ATP. In biochemical assays, the inhibitory effect of ON01910 was unaffected (IC_{50} remain to be 9–10 nM) with escalating ATP concentrations[23,24].

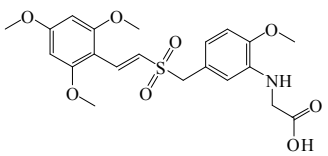

Figure 10. Chemical structure of ON01910 (compound **16**).

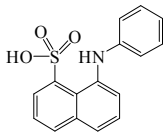

Figure 11. Chemical structure of ANS (compound **17**).

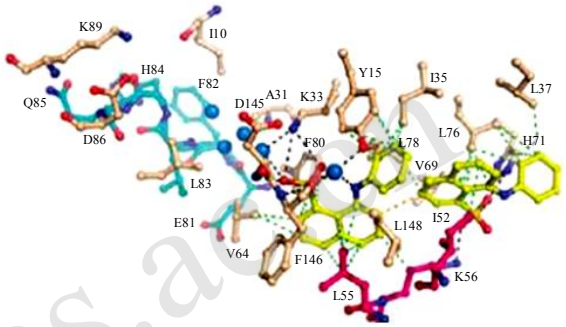

Figure 12. X-ray co-crystal structure of ANS binds to CDK2 (PDB ID2CCI). Black and green dotted lines indicate hydrogen bonding and hydrophobic interactions, respectively. Water molecules are shown as blue spheres[25].

2.4. Cyclin-dependent kinases inhibitors

Cyclin-dependent kinases (CDKs) belong to the CMGC class of serine/threonine protein kinases that act as key regulatory elements in cell cycle progression. They are also involved in regulating transcription, mRNA processing, and the differentiation of nerve cells. Dysregulation of CDKs has been implicated in a number of diseases, especially in various forms of cancer. By definition, a CDK binds a regulatory protein called a cyclin to form the cyclin-CDK complex which is the active kinase catalyzing the phosphorylation of downstream kinases. Without cyclin bound, CDK alone has little kinase activity. Therefore, interrupting the binding between CDKs and cyclins can potentially be an effective, allosteric way to modulate CDKs activity.

ANS (Fig. 11) interacts with free CDK2, but not with cyclin A, to produce a characteristic fluorescence spectrum. Fluorescence intensity decreased in a dose-dependent manner upon interaction with cyclin A but not with substrate ATP. The crystal structure of the CDK2-ANS complex revealed two distinct ANS molecules bound adjacent to one another, away from the ATP site and in the vicinity of the C-helix (Fig. 12). They induce large structural changes in CDK2 not previously observed with small molecule ligands of this enzyme. The C-helix is locked in a conformation substantially different from that of CDK2 alone or in complex with cyclin[25]. One ANS molecule binds to a site midway between the ATP site and the C-helix, defined as the primary ANS site. The naphthalene ring is positioned between C-helix residues Leu55 and Lys56 and gatekeeper residue Phe80. The sulfonate group is within hydrogen bonding distance of the main chain amides of Asp145 and Phe146, which constitute the DFG motif, and appears to establish a salt bridge with the ε-amino group of the conserved Lys33 residue. The second ANS molecule binds adjacent to the primary site, within van der Waals distance of the first ANS molecule. This secondary site is also composed of C-helix residues. The naphthalene is located between residues Ile52 and Leu76, and the sulfonate group interacts with residues Lys56 and His71, while the aniline moiety is largely solvent exposed. The ANSs appear to be competitive with cyclin and are readily displaced by cyclin due to their low affinity (K_d = 37 μM). A larger ligand that is capable of fully utilizing the binding site of both ANS molecules should produce much higher potency and be more effective for competition with cyclin.

2.5. Aurora kinases inhibitors

Aurora kinases are serine/threonine kinases that play an integral role in cell proliferation. The kinases help the

dividing cells dispense their genetic materials to daughter cells. More specifically, Aurora kinases play a crucial role in cellular division by controlling chromatid segregation. Defects in this segregation can cause genetic instability, a condition which is highly associated with tumorigenesis[26]. Three Aurora kinases (Aurora-A, B, and C) have been identified in mammalian cells to date. Besides being implicated as mitotic regulators, these three kinases have generated significant interest in the cancer research field due to their elevated expression profiles in many human cancers[27].

Compound **18** (Fig. 13) is an early lead compound from Amgen that showed good inhibitory activities against both Aurora-A and B in enzymatic assays but exhibited poor cellular activity. Further structural modification led to the discovery of the anthranilamide derivative **19** (Fig. 13). It is also a dual aurora inhibitor that displays potent cellular activity (EC_{50} = 15 nM) and good kinase selectivity.

The difference in cellular activity and kinase selectivity observed between compounds **18** and **19** was attributed to their different binding modes to the Aurora-A kinase. X-ray crystallographic data show **18** binds to Aurora-A (Fig. 13a, PDB ID: 3O50) with the activation loop in the DFG-in conformation and the trifluoromethyl substituent on the phenyl ring is surrounded by lipophilic side-chains of Val174 and Ile178 in the C-helix and Phe144 in the P-loop. Compound **18** forms several key hydrogen-bonding interactions, including the pyrimidine nitrogen and kinase hinge NH (Ala213), the amide carbonyl and the amino terminus of the catalytic lysine (Lys162), and the amide NH of **18** and the side chain of Asn261 (water-mediated). The co-crystal structure of **19**/Aurora-A complex (PDB ID: 3O51) shows the pyrimidine-pyridine-*O*-phenyl portion of **19** making similar contacts in the ATP-binding site. But the conserved DFG motif of the activation loop occupies a strikingly different DFG-out conformation, with the aromatic ring of the anthranilamide partially occupying the space vacated by Phe275 and the terminal phenyl ring flanked by lipophilic side-chain residues of the C-helix (Val174 and Ile178) and P-loop (Phe144). The anthranilamide adopts an internally hydrogen bonded conformation, with the plane of the amide nearly parallel to Phe275. The movement of the kinase activation loop in the Aurora-A/**19** co-crystal structure (Fig. 13) appears to be induced by the anthranilamide, as the *N*-phenyl portion of the molecule is incompatible with the DFG-in conformation[28].

2.6. B-Rafkinase allosteric inhibitors

Raf kinases belong to serine/threonine kinase family and are consisted of three isoforms, A-Raf, B-Raf, and C-Raf (Raf-1). Activated Raf kinase triggers the phosphorylaton/activation of the MEK and ERK cascade, which plays important roles in cell proliferation and survival[29]. In particular, B-Raf kinase has emerged as one of the most attractive molecular targets for cancer therapy because somatic mutations of B-Raf have frequently been found in human tumors[30]. Activating somatic mutations of B-Raf have been observed in about 60% of melanomas, 40% of thyroid cancer, 20% of colon and ovarian cancer. The crystal structure of B-Raf shows an intramolecular interaction between the glycine-rich loop and the activation segment, which helps to maintain an inactive status of B-Raf. V600E which is the most common B-Raf mutation in its catalytic domain causes the breakage of this intramolecular interaction and constitutive activation of B-Raf[31].

Sorafenib (Fig. 14) was shown to potently inhibit the kinase activity of wild-type B-Raf as well as oncogenic B-Raf V600E mutant[32]. The X-ray co-crystal structure (Fig. 15) reveals that sorafenib bound to the DFG-out conformation of B-Raf V600E mutant[31].The backbone of Cys532 in the hinge region interacts with the nitrogen of the 4-pyridyl group and the methylamide group of sorafenib. The aromatic stacking interaction (π–π interaction) is observed between the pyridyl ring of sorafenib and Trp531 of the hinge region/Phe583 at the catalytic loop/Phe595 of the DFG motif. The urea group of sorafenib makes a pair of hydrogen bonds with Asp594 backbone of the DFG loop and Glu501 side chain of the αC-helix, respectively. The lipophilic trifluoromethyl group of sorafenib occupies a hydrophobic pocket composed of Thr507, Ilu512 and Leu566.

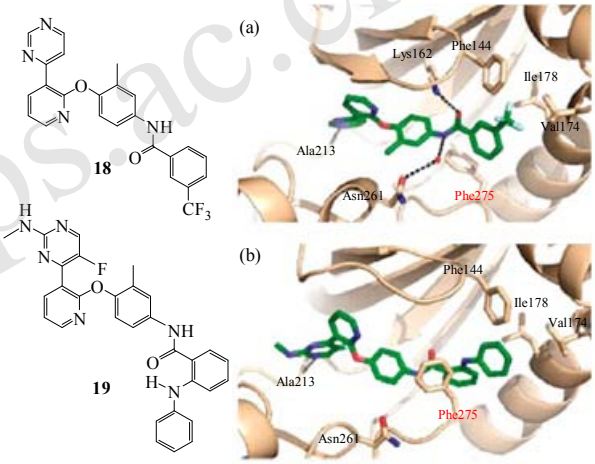

Figure 13. X-ray co-crystal structure of compounds **18** and **19** binds to the kinase domain of Aurora-A[27].

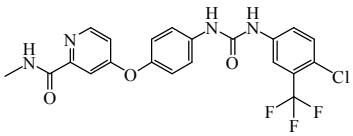

Figure 14. Chemical structure of sorafenib (compound **20**).

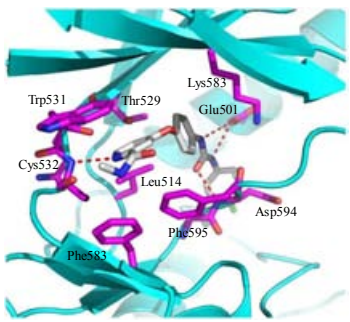

Figure 15. X-ray co-crystal structure of sorafenib bound to the kinase domain of B-Raf V600E mutant (PDB code: 1UWH).

2.7. Checkpoint kinase 1 inhibitors

In the setting of DNA damage, inhibition of checkpoint kinases can lead to genomic instability, and subsequent cell death. The first checkpoint, found at the G1/S transition, is compromised in many malignant cells, due to mutations in various tumor suppressor genes, including retinoblastoma protein (Rb) and p53. Cells deficient in the G1 checkpoint are dependent on the S and G2 checkpoints for DNA repair. Checkpoint kinase-1 (CHK1) is an active transducer kinase at both the S and G2 checkpoints, rendering it a target for rational anticancer drug development. In the presence of DNA damage, CHK1 inactivation abrogates G2 arrest, resulting in preferential cancer cell death[33]. Allosteric inhibitors of CHK1 kinase are listed in Table 4.

Thioquinazolinone **21** (Table 4) inhibits the CHK1 through allosteric binding to a shallow hydrophobic groove of the kinase. The X-ray co-crystal structure showed that compound **21** bound ~13 Å away from ATP binding site. The spiropiperidine amine is engaged in two direct hydrogen bonding contacts with the carboxylic acid of Glu205 and the backbone amide nitrogen of Leu206. The thioquinazolinone carbonyl oxygen participates in a water mediated hydrogen bond to Glu134. The *p*-chlorophenylquinazolinone occupies a hydrophobic pocket formed by Phe93, Ile96, Pro133, and Leu206, forming α-interaction (Fig. 16). Although, compound **21** is a relatively weak inhibitor against CHK1 with IC_{50} = 1.3 μM, but its allosteric binding mode provides a good starting points for the development of potent and selective CHK1 inhibitors[34].

Compounds **22** and **23** (Table 4) have been shown to be inhibitors of CHK1 with K_i of 1.89 μM and 0.15 μM. Co-crystal structures of compounds **22** and **23** with CHK1 show similar binding mode as that of thioquinazolinone **21** (Fig. 17). This site includes a hydrophobic pocket formed by the side chains of Phe93, Pro133, Leu206, and Ala200, along with side chains from the IEPDIG motif. This hydrophobic pocket has been proposed as the P-5 substrate binding site. The conserved PDIG motif limits the RD helix to a single turn, resulting in a shallow groove that wraps around the IEPDIG loop and merges with the hydrophobic pocket. Both compounds fill the pocket and a portion of the groove. For compound **22**, the dichlorophenyl motif occupies the lipophilic P-5 pocket. The phenyl side chain of Phe93 allows for some buried hydrophobic surface contact with the dichlorophenyl portion of the inhibitor. The NH group of the carbamate and the benzimidazole 1-NH group form hydrogen bonds with the backbone carbonyl groups of Phe93 and Asp94, respectively. The chiral methyl is in the *S*-configuration and is also making a hydrophobic interaction with the backbone and side chain of Asp94. The carbamate is binding in the shallow surface groove that wraps around the IEPDIG loop. The face of the benzimidazole group makes contact with the backbone and side chains of Glu97 and Pro98. Compound **23** binds in the same orientation as compound **22** but establishes two additional hydrogen bonds and makes more extensive hydrophobic surface contact. A water-mediated hydrogen bond is formed between the nitro oxygen of the inhibitor and the hydroxy group of the Tyr173 side chain. There is significant hydrophobic surface contact between

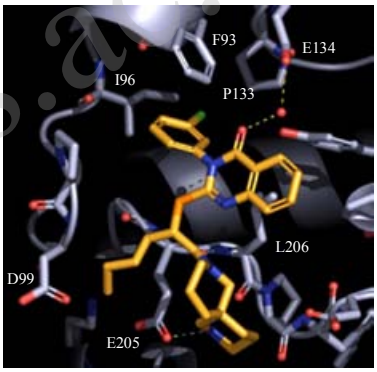

Figure 16. X-ray co-crystal structure of compound **21** (gold) binds to CHK1. Direct hydrogen bonding contacts to the carboxylic acid of Glu205 and the backbone amide nitrogen of Leu206 are shown in white dashes. Water mediated hydrogen bond to Glu134 is shown as a yellow dash[34].

Table 4. Allosteric inhibitors of CHK1 kinase

Comp.	Anonym	Structure	Target IC_{50} (M)[a]	Status	Institute
21	Compound **21**	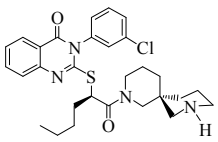	1.3	Preclinical	Merck
22	Compound **22**	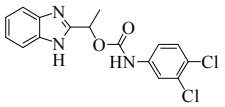	1.89	Preclinical	Pfizer
23	Compound **23**	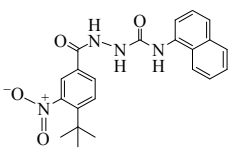	0.15	Preclinical	Pfizer

[a] Enzymatic activity assay.

the *tert*-butyl substituent and the backbone and side chains of Leu206 and Ala200 and the Glu205 backbone. Hydrogen bonding also exists between the 2-NH group of the hydrazide group and the carbonyl of Phe93, as well as between the 1-amino substituent of the naphthalene and the carbonyl of Ile96. The face of the naphthyl group interacts with the backbone and side chains of Glu97 and Pro98. The additional ligand-protein hydrogen bonds and increased hydrophobic surface contact of compound **23** may account for its increased binding affinity relative to that of compound **22**[35].

2.8. Phosphoinositide-dependent kinase 1 inhibitors

Phosphoinositide-dependent kinase 1 (PDK1) was a protein serine/threonine kinase that linked to phosphatidylinositol 3 kinase (PI3K) to AKT (protein kinase B) activation in response to growth factor receptor signaling. PDK1 has been shown to phosphorylate about 20 related protein kinases, therefore, been referred to as the "master regulator" of the AGC protein kinase family[36]. The observation that several kinases phosphorylated by PDK1 are positioned in the oncogenic PI3K- or MAPK-signaling pathways and are themselves oncology targets (i.e. AKT, RSK (p90 ribosomal S6 kinase), PKC, and p70S6K (p70 ribosomal S6 kinase)) has prompted the development of small molecule PDK1 inhibitors. Since pathological activation of the PI3K pathway has been related to the growth of tumor cells, inhibition of PDK1 is predicted to inhibit oncogenic cellular processes and thus be therapeutically beneficial.

Compound **24** (Fig. 18) has been identified as a potent (IC_{50} = 1 nM) and selective (>3000 fold against a 256-kinase panel) PDK1 inhibitor. It uniquely binds to the inactive kinase conformation (DFG-out) of PDK1 in a similar fashion as imatinib binds to Bcr-Abl, and inhibits the cellular phosphorylation of PDK1 at Ser-241. Like imatinib, compound **24** can be sectioned into three molecular fragments: a hinge binding group, a linker, and a hydrophobic moiety. The hinge binding group extends into the ATP pocket and establishes H-bond interactions with the hinge. The hydrophobic moiety, which occupies a pocket only present in the inactive conformation of PDK1, engages residues in PDK1 that are not conserved broadly within the kinase super family, contributing to both its high potency and selectivity (Fig. 19). Compound **24** additionally disrupts the αC-helix, a feature unique to this type of inhibitors specifically interacting with the inactive form of PDK1. The conformational change in the αC-helix results in catalytic residue Glu-130 being displaced from the active site rendering it inactive[37].

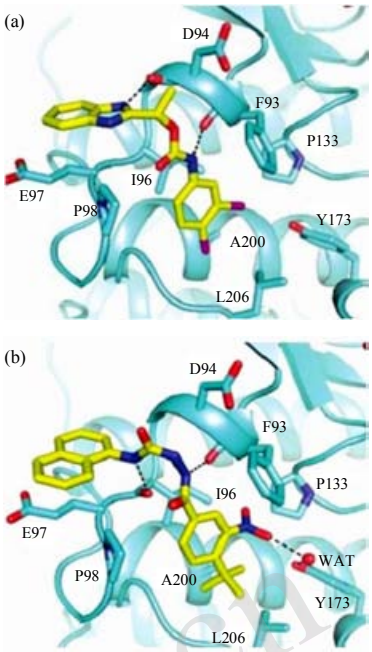

Figure 17. X-ray co-crystal structure of compounds **22** (a, yellow) and **23** (b, yellow) binds to CHK1[35].

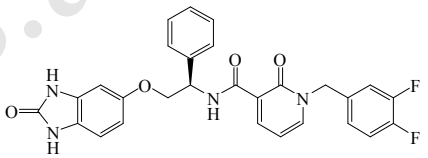

Figure 18. Chemical structure of compound **24**.

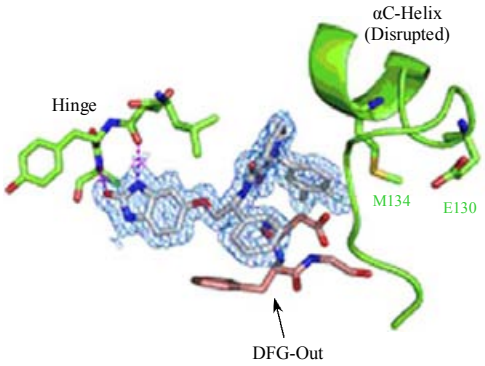

Figure 19. X-ray co-crystal structure of compound **24** binds to PDK1[37].

3. Conclusions

During the past two decades, tremendous efforts have been invested in understanding the intricacy of the kinase network responsible for signal transduction and discovering safe and effective ways to modulate their activities. To this end, fifteen distinct small-molecule kinase inhibitors have received US Food and Drug Administration approval for the treatment of specific cancers. This not only charts the routes for discovering new kinase inhibitor drugs but also reveals challenges in this field. The discovery of potent and selective kinase inhibitors that can achieve clinical safety and efficacy remain to be difficult. The emerging drug resistance due to mutations also makes a specific kinase inhibitor less effective. For these reasons, allosteric kinase inhibitors continue to be the focus of many research programs because of their specific binding sites, excellent selectivity profile and slow kinetics (slow

disassociation from the kinase, therefore, prolonged target occupancy). However, so far, the allosteric inhibitors of the majority of kinases remain to be discovered. In addition, it is impossible to predict, according their amino acids sequence, the allosteric conformation or allosteric binding sites which can affect their catalytic activity after binding with a ligand. The presence of a small molecule ligand may be a requirement to induce, bind to and stabilize the allosteric conformation or sites. Therefore, there is a compelling need to expand the chemical space available for synthesizing new, potent and selective kinase inhibitors which can modulate their targets' activity allosterically. Structure based drug design techniques using the X-ray crystal structure of the kinase and their bound inhibitors have made and will continue to make meaningful contribution in the discovery and optimization of novel allosteric inhibitors. We hypothesize that rationally designed inhibitors based on the Type 2 pharmacophore will allow the generation of high-affinity inhibitors that can stabilize the allosteric conformation of many other kinases for which this conformation has not yet been observed. In addition to serving as lead compounds for drug discovery and as tools to investigate signaling pathways, these new Type 2I kinase inhibitors will allow the structural plasticity of the kinases to be more fully explored.

References

[1] Zhang, J.M.; Yang, P.L.; Gray, N.S. *Nat. Rev. Cancer*. **2009**, *9*, 28–39.

[2] Zhang, C.; Bollag, G. *Curr. Opin. Genet. Dev.* **2010**, *20*, 79–86.

[3] Liu, Y.; Gray, N.S. *Nat. Chem. Biol.* **2006**, *2*, 358–364.

[4] Dietrich, J.; Hulme, C.; Hurley, L.H. *Bioorg. Med. Chem. Lett*. **2010**, *18*, 5738–5748.

[5] Nagar, B.; Bornmann, W.G.; Pellicena, P. *Cancer Res*. **2002**, *65*, 4236–4243.

[6] Hassan, A.Q.; Sharma, S.V.; Warmuth, M. *Cell Cycle*. **2010**, *9*, 3170–3174.

[7] Choi, H.G.; Ren, P.D.; Adrian, F.; Sun, F.X.; Lee, H.S.; Wang, X.; Ding, Q.; Zhang, G.B.; Xie, Y.P.; Zhang, J.M.; Liu, Y.; Tuntland, T.; Warmuth, M.; Manley, P.W.; Mestan, J.; Gray, N.S.; Sim, T. *J. Med. Chem*. **2010**, *53*, 5439–5448.

[8] Okram, B.; Nagle, A.; Adria, F.J.; Lee, C.; Ren, P.D.; Wang, X.; Sim, T.; Xie, Y.P.; Wang, X.; Xia, G.; Spraggon, G.; Warmuth, M.; Liu, Y.; Gray, N.S. *Chem. Biol.* **2006**, *13*, 779–786.

[9] Zhang, J.M.; Adrián, F.J.; Jahnke, W.; Cowan-Jacob, S.W.; Li, A.G.; Iacob, R.E.; Sim, T.; Powers, J.; Dierks, C.; Sun, F.X.; Guo, G.R.; Ding, Q.; Okram, B.; Choi, Y.; Wojciechowski, A.; Deng, X.M.; Liu, G.X.; Fendrich, G.; Strauss, A.; Vajpai, N.; Grzesiek, S.; Tuntland, T.; Liu, Y.; Bursulaya, B.; Azam, M.; Manley, P.W.; Engen, J.R.; Daley, G.Q.; Warmuth, M.; Gray, N.S. *Nature*. **2010**, *463*, 501–507.

[10] Bogoyevitch, M.A.; Fairlie, D.P. *Drug Discov. Today*. **2007**, *12*, 622–633.

[11] Pargellis, C.; Tong, L.; Churchill, L.; Cirillo, P.F.; Gilmore, T.; Graham, A.G.; Grob, P.M.; Hickey, E.R.; Moss, N.; Pav, S.; Regan, J. *Nat. Struct. Biol.* **2002**, *9*, 268–272.

[12] Cumming, J.G.; McKenzie, C.L.; Bowden, S.G.; Campbell, D.; Masters, D.J.; Breed, J.; Jewsbury, P.J. *Bioorg. Med. Chem. Lett*. **2004**, *14*, 5389–5394.

[13] Gill, A.L.; Frederickson, M.; Cleasby, A.; Woodhead, S.G.; Carr, M.G.; Woodhead, A.G.; Walker, M.T.; Congreve, M.S.; Devine, L.A.; Tisi, D.; O'Reilly, M.; Seavers, L.C.A.; Davis, D.J.; Curry, J.; Anthony, R.; Padova, A.; Murray, C.W.; Carr, R.A.E.; Jhoti, H. *J. Med. Chem*. **2004**, *48*, 414–426.

[14] Hynes, J.Jr.; Dyckman, A.J.; Lin, S.Q.; Wrobleski, S.T.; Wu, H.; Gillooly, K.M.; Kanner, S.B.; Lonial, H.; Loo, D.; McIntyre, K.W.; Pitt, S.; Shen, D.R.; Shuster, D.J.; Yang, X.X.; Zhang, R.; Behnia, K.; Zhang, H.Z.; Marathe, P.H.; Doweyko, A.M.; Tokarski, J.S.; Sack, J.S.; Pokross, M.; Kiefer, S.E.; Newitt, J.A.; Barrish, J.C.; Dodd, J.; Schieven, G.L.; Leftheris, K. *J. Med. Chem*. **2007**, *51*, 4–16.

[15] Liu, C.J.; Lin, J.; Wrobleski, S.T.; Lin, S.Q.; Hynes, J.; Wu, H.; Dyckman, A.J.; Li, T.L.; Wityak, J.; Gillooly, K.M.; Pitt, S.; Shen, D.R.; Zhang, R.F.; McIntyre, K.W.; Salter-Cid, L.; Shuster, D.J.; Zhang, H.J.; Marathe, P.H.; Doweyko, A.M.; Sack, J.S; Kiefer, S.E.; Kish, K.F.; Newitt, J.A.; McKinnon, M.; Dodd, J.H.; Barrish, J.C.; Schieven, G.L.; Leftheris, K. *J. Med. Chem*. **2010**, *53*, 6629–6639.

[16] Sebolt-Leopold, J.S.; Herrera, R. *Nat. Rev. Cancer*. **2004**, *4*, 937–947.

[17] McCubrey, J.A.; Milella, M.; Tafuri, A.; Martelli, A.M.; Lunghi, P.; Bonati, A.; Cervello, M.; Lee, J.T.; Steelman, L.S. *Curr. Opin. Invest. Drugs*. **2008**, *9*, 614–630.

[18] Fremin, C.; Meloche, S. *J. Hematol. Oncol*. **2010**, *3*, 8. doi: 10.1186/1756-8722-3-8

[19] Ohren, J.F.; Chen, H.F.; Pavlovsky, A.; Whitehead, C.; Zhang, E.L.; Kuffa, P.; Yan, C.H.; McConnell, P.; Spessard, P.; Banotai, C.; Mueller, W.T.; Delaney, A.; Omer, C.; Sebolt-Leopold, J.; Dudley, D.T.; Leung, I.K.; Flamme, C.; Warmus, J.; Kaufman, M.; Barrett, S.; Tecle, H.; Hasemann, C.A. *Nat. Struct. Mol. Biol.* **2004**, *11*, 1192–1197.

[20] Iverson, C.; Larson, G.; Lai, C. *Cancer Res*. **2009**, *69*, 6839–6847.

[21] Dong, Q.; Dougan, D.R.; Gong, X.C.; Halkowycz, P.; Jin, B.H.; Kanouni, T.; O'Connell, S.M.; Scorah, N.; Shi, L.H.; Wallace, M.B.; Zhou, F. *Bioorg. Med. Chem. Lett*. **2011**, *21*, 1315–1319.

[22] Isshiki, Y.; Kohchi, Y.; Iikura, H.; Matsubara, Y.; Asoh, K.; Murata, T.; Kohchi, M.; Mizuguchi, E.; Tsujii, S.; Hattori, K.; Miura, T.; Yoshimura, Y.; Aida, S.; Miwa, M.; Saitoh, R.; Murao, N.; Okabe, H.; Belunis, C.; Janson, C.; Lukacs, C.; Schück, V.; Shimma, N. *Bioorg. Med. Chem. Lett*. **2011**, *21*, 1795–1801.

[23] Kirkland, L.O.; McInnes, C. *Biochem.Pharmcol.* **2009**, *77*, 1561–1571.

[24] Beria, I.; Valsasina, B.; Brasca, M.G.; Ceccarelli, W.; Colombo, M.; Cribioli, S.; Fachin, G.; Ferguson, R.D.; Fiorentini, F.; Gianellini, L.M.; Giorgini, M.L.; Moll, J.K.; Posteri, H.; Pezzetta, D.; Roletto, F.; Sola, F.; Tesei, D.; Caruso, M. *Bioorg. Med. Chem. Lett.* **2010**, *20*, 6489–6494.

[25] Betzi, S.; Alam, R.; Martin, M.; Lubbers, D.J.; Han, H.J.; Jakkaraj, S.R.; Georg, G.I.; Schonbrunn, E. *ACS Chem. Biol.* **2011**, *6*, 492–501.

[26] Bolanos-Garcia, V.M. *Cell Biology.* **2005**, *37*, 1572–1577.

[27] Giet, R.; Prigent, C. *J. Cell. Sci.* **1999**, *112*, 3591–3601.

[28] Cee, V.J.; Schenkel, L.B.; Hodous, B.L.; Deak, H.L.; Nguyen, H.N.; Olivieri, P.R.; Romero, K.; Bak, A.; Be, X.H.; Bellon, S.; Bush, T.L.; Cheng, A.C.; Chung, G.; Coats, S.; Eden, P.M.; Hanestad, K.; Gallant, P.L.; Gu, Y.; Huang, X.; Kendall, R.L.; Lin, M.J.; Morrison, M.J.; Patel, V.F.; Radinsky, R.; Rose, P.E.; Ross, S.; Sun, J.R.; Tang, J.; Zhao, H.L.; Payton, M.; Geuns-Meyer, S.D. *J. Med. Chem.* **2010**, *53*, 6368–6377.
[29] Yoon, S.; Seger, R. *Growth Factors*. **2006**, *24*, 21–24.
[30] Garnett, M.J.; Marais, R. *Cancer Cell.* **2004**, *6*, 313–319.
[31] Wan, P.T.C.; Garnett, M.J.; Roe, S.M.; Lee, S.; Niculescu-Duvaz, D.; Good, V.M.; Jones, C.M.; Marshall, C.J.; Springer, C.J.; Barford, D.; Marais, R. *Cell*. **2004**, *116*, 855–867.
[32] Wilhelm, S.M.; Carter, C.; Tang, L.Y.; Wilkie, D.; McNabola, A.; Rong, H.; Chen, C.; Zhang, X.M.; Vincent, P.; McHugh, M.; Cao, Y.C.; Shujath, J.; Gawlak, S.; Eveleigh, D.; Rowley, B.; Liu, L.; Adnane, L.; Lynch, M.; Auclair, D.; Taylor, I.; Gedrich, R.; Voznesensky, A.; Riedl, B.; Post, L.E.; Bollag, G.; Trail, P.A. *Cancer Res.* **2004**, *64*, 7099–7109.
[33] Chen, Z.H.; Xiao, Z.; Chen, J.; Ng, S.C.; Sowin, T.; Sham, H.; Rosenberg, S.; Fesik, S.; Zhang, H.Y. *Mol. Cancer Ther.* **2003**, *2*, 543–548.
[34] Converso, A.; Hartingh, T.; Garbaccio, R.M.; Tasber, E.; Rickert, K.; Fraley, M.E.; Yan, Y.W.; Kreatsoulas, C.; Stirdivant, S.; Drakas, B.; Walsh, E.S.; Hamilton, K.; Buser, C.A.; Mao, X.Z.; Abrams, M.T.; Beck, S.C.; Tao, W.K.; Lobell, R.; Sepp-Lorenzino, L.; Zugay-Murphy, J.; Sardana, V.; Munshi, S.K.; Jezequel-Sur, S.M.; Zuck, P.D.; Hartman, G.D. *Bioorg. Med. Chem. Lett*. **2009**, *19*, 1240–1244.
[35] Vanderpool, D.; Johnson, T.O.; Ping, C.; Bergqvist, S.; Alton, G.; Phonephaly, S.; Rui, E.; Luo, C.; Deng, Y.L.; Grant, S.; Quenzer, T.; Margosiak, S.; Register, J.; Brown, E.; Ermolieff, J. *Biochemistry*. **2009**, *48*, 9823–9830.
[36] Mora, A.; Komander, D.; Aalten, D.M.F.; Alessi, D.R. *Semin. Cell Dev. Biol*. **2004**, *15*, 161–170.
[37] Nagashima, K.; Shumway, S.D.; Sathyanarayanan, S.; Chen, A.H.; Dolinski, B.; Xu, Y.Y.; Keilhack, H.; Nguyen, T.; Wiznerowicz, M.; Li, L.X.; Lutterbach, B.A.; Chi, A.; Paweletz, C.; Allison, T.; Yan, Y.W.; Munshi, S.K.; Klippel, A.; Kraus, M.; Bobkova, E.V.; Deshmukh, S.; Xu, Z.W.; Mueller, U.;Szewczak, A.A.; Pan, B.S.; Richon, V.; Pollock, R.; Blume-Jensen, P.; Northrup, A.; Andersen, J.N. *J. Biol. Chem.* **2011**, *286*, 6433–6448.

激酶变构抑制剂: 一种新的高效和高选择性调节激酶活性的方式

杨洪亮, 陈婷, 柏旭, 裴亚中*

吉林大学 药学院 组合化学与创新药物研究中心, 吉林 长春 130021

摘要: 研究证明, 激酶活性失控是导致癌症的原因之一, 癌细胞存活和增殖与相应激酶活性的失控密切相关。选择性的抑制激酶活性已经成为开发安全有效的抗癌药的重点研究领域。到目前为止, 已有15种激酶抑制剂得到美国食品药品监督管理局的批准用于治疗多种癌症。其中, 激酶的变构抑制剂在临床上显示出更好的安全性和有效性。本文将总结这些激酶的变构构象、它们对应的抑制剂及其作用方式。

关键词: 蛋白激酶; 变构构象; DFG-out; ATP非竞争性; 激酶抑制剂

Dr. Yazhong Pei received his degree of Bachelor of Science from the Department of Chemistry of Jilin University in 1984 and his Ph.D. degree in Organic Chemistry from The State University of New York at Stony Brook in 1990. Since then he has worked in the pharmaceutical and biotech industry in the United States of America focusing the design and synthesis of novel small molecules as therapeutic agents for various diseases, especially in the areas of oncology and auto-immune disorders. Recently, he served as the Director of Chemistry at CalciMedica, a biotech company in San Diego. Previously, he worked at several other San Diego biotech companies including Kemia, MitoKor, and Trega Biosciences in various drug discovery and development management roles. Currently, he is the Aoqing Tang Professor at The Center for Combinatorial Chemistry and Drug Discovery and the School of Pharmaceutical Sciences of Jilin University.

裴亚中博士, 1984年毕业于吉林大学化学系, 获理学学士学位; 1990年毕业于美国纽约州立大学, 获化学博士学位。裴亚中博士拥有二十余年在美国制药工业界的工作经验, 致力于创新药物的设计和合成。他参与和领导了涉及多种疾病领域, 如自身免疫失调和癌症的新药研发项目。曾在Kemia公司担任药物化学部副主任, MitoKor公司担任药物化学部主任。现任美国圣地亚哥CalciMedica, Inc. 公司的化学部主任。2010年3月至今任吉林大学组合化学与创新药物研究中心和药学院唐敖庆特聘教授、博士生导师。